2026 年研究生国家奖学金个人情况统计表

姓名	王悦	性别		政治面貌	
学院	古生物学院	专业名称	生物学	学号	
入学时间		身份证号			

项目类别	论文题目或相应名称	刊物名称或审批单位	时间	备注
论文	A new species of *Nilssoniopteris* (Bennettitales) from the Lower Cretaceous Jianchang Basin, western Liaoning, NE China. （中科院三区）	Review of Palaeobotany and Palynology	2026 年 8 月	第一作者
科研立项	辽西中生代本内苏铁类植物化石的全球三维重建与古气候协同模拟研究	辽宁省教育厅	2025 年 6 月	参与

注：1.上述内容应严格按照评选细则如实填写，如发现所填内容与实际不符，将取消评选资格。

2.表格应严格按照填表要求规范填写。

3.备注栏中填写作者（获奖）顺序。

Review of Palaeobotany and Palynology 355 (2026) 105703

Contents lists available at ScienceDirect

Review of Palaeobotany and Palynology

journal homepage: www.elsevier.com/locate/revpalbo

Research papers

A new species of *Nilssoniopteris* (Bennettitales) from the Lower Cretaceous Jianchang Basin, western Liaoning, NE China

Yue Wang [a], Xiao Tan [a,b,*], Jiayi Zhang [a], Rui He [a], Mengyang Zhang [c], Fei Liang [a,b], Yunfeng Li [d,e], Chunlin Sun [d,e]

[a] College of Paleontology, Shenyang Normal University, Shenyang 110034, Liaoning Province, China
[b] Key Lab of Evolution of Past Life in NE Asia, Ministry of Natural Resources, Shenyang Normal University, Shenyang 110034, Liaoning Province, China
[c] Liaoning Natural Resources Affairs Service Center, Shenyang 110032, Liaoning Province, China
[d] Research Center of Paleontology and Stratigraphy, Jilin University, Changchun 130026, Jilin Province, China
[e] College of Earth Sciences, Jilin University, Changchun 130061, Jilin Province, China

ARTICLE INFO

Keywords:
Bennettitales
Nilssoniopteris
Early Cretaceous
Jianchang Basin
Paleoclimate
Paleobiogeography

ABSTRACT

The Bennettitales were a prevalent Mesozoic plant group that became extinct at the end of the Cretaceous. *Nilssoniopteris*, an important bennettitalean genus, differs from other fossil genera and extant cycads by its entire-margined leaves and syndetocheilic stomata with sinuous cell walls. The genus was distributed mainly across mid-latitude regions of Eurasia and North America from the Late Triassic to the Early Cretaceous, and is generally considered an indicator of warm, humid climates. Here we report a new fossil species, *Nilssoniopteris macrophylla* sp. nov., from the Lower Cretaceous Binggou Formation of the Jianchang Basin, western Liaoning, China. This specimen represents one of the largest known leaves of the genus to date. We describe its macroscopic morphology and epidermal structure in detail. Together with the co-occurring species *N. binggouensis* Na et al., this discovery marks the easternmost distribution of the genus in Eurasia. A compilation of global occurrences of *Nilssoniopteris* reveals a pronounced northward migration from the Triassic to the Cretaceous, culminating in its appearance at mid-to-high paleolatitudes during the Albian. The leaf size and entire margin of *N. macrophylla* are consistent with warm, frost-free, and humid climatic conditions that prevailed during the late Albian. The occurrence of this species at 106.5 ± 1.9 Ma, falling within the OAE 1b–c interval, provides terrestrial evidence that the greenhouse warming associated with these oceanic anoxic events also affected continental ecosystems in Northeast China, enabling thermophilic plants to expand into higher latitudes.

1. Introduction

Bennettitales, an extinct group of gymnosperms, flourished from the Middle Triassic to Late Cretaceous, broadly coinciding with the main era of dinosaur dominance (Bomfleur et al., 2018; Rudall and Bateman, 2019). The earliest known leaf fossils with well-preserved epidermal structures appeared in the Early Permian, predating their major diversification in the Mesozoic (Blomenkemper et al., 2021). The group then became widespread and dominant in many floras from the Triassic to the Early Cretaceous, before gradually declining and finally disappearing by the end of Cretaceous. Several genera, particularly the leaf-form genera of the group such as *Pterophyllum* Brongniart, *Anomozamites* Shimper emend. Harris, *Otozamites* Braun, et al. and *Nilssoniopteris* Nathorst, formed significant component of Mesozoic floras worldwide (Florin, 1933; Sze, 1936; Harris, 1969; Pott et al., 2007; Taylor et al., 2009). Although most genera of the Bennettitales are preserved as isolated compressed foliage, and their forms are often difficult to distinguish from those of Cycadales based on macromorphology, their epidermal structures, namely syndetocheilic stomata and distinctly sinuate cell walls, can be readily identified.

Nilssoniopteris Nathorst, as a leaf-form genus of Bennettitales, is considered to represent an early evolutionary stage toward lobed leaves, characterized by its entire, essentially undissected pinnate lobes (Mamay, 1976). The epidermal cells of typical *Nilssoniopteris* usually have sinuous anticlinal walls, although some Triassic forms exhibit straight walls, such as *N. lunzensis* from the Carnian of Austria (Pott et al., 2007). Morphologically similar strap-shaped leaves with haplocheilic stomata are assigned to *Doratophyllum* Harris, whereas

* Corresponding author.
E-mail address: tanxiao1115@163.com (X. Tan).

https://doi.org/10.1016/j.revpalbo.2026.105703
Received 10 June 2026; Received in revised form 4 August 2026; Accepted 13 August 2026
Available online 20 August 2026

comparable Paleozoic leaves lacking epidermal preservation are often classified as *Taeniopteris* Brongniart (Sze and Li, 1963; Taylor et al., 2009). Thus, *Nilssoniopteris* can be clearly distinguished by the combination of pinnately lobed leaves, lobes with entire-margined leaf, syndetocheilic stomata, and sinuous cell walls.

The genus was first described by Nathorst (1909) based on Jurassic material from Yorkshire and is primarily distributed across Eurasia (Harris, 1969), with very few reliable reports from North America and the Southern Hemisphere. Its oldest record is from the Late Triassic Carnian flora from Lunz, Lower Austria (Pott et al., 2007). During the Jurassic, *Nilssoniopteris* was widespread and common in the North Hemisphere floras, with records from Sweden and Great Britain (Nathorst, 1909; Lundblad, 1950; Harris, 1969; Watson and Sincock, 1992), Iran and Afghanistan (Sadovnikov, 1989; Schweitzer and Kirchner, 2003), China (Chen et al., 1984; Wang, 1984; Zhang, 1984; Li et al., 1988; Sun and Shen, 1988; Sun and Yang, 1988; Wei et al., 2005), and Greenland (Harris, 1932; Boyd, 2000). During the Cretaceous, however, the distribution of *Nilssoniopteris* because more restricted to northern regions, including Hebei, Liaoning, Jilin provinces, as well as Inner Mongolia in China (Wang, 1984; Chen et al., 1988; Zheng et al., 1990; Deng, 1995; Wei et al., 2005; Na et al., 2014; Li, 2017), Russia (Samylina, 1964, 1976), Mongolia (Herrera et al., 2018), Canada (Ray et al., 2014), and southwestern Japan (Yamada et al., 2009). The youngest geological records of *Nilssoniopteris* include *N. pecinovensis* from the Cenomanian the Upper Cretaceous in the Czech Republic (Kvaček, 1995) and *Nilssoniopteris* sp. from the Upper Cretaceous in New Zealand (Parrish et al., 1998).

The occurrence of *Nilssoniopteris* is generally regarded as an indicator of warm and humid subtropical to temperate climates. Insights from its nearest living relatives, the cycads, suggest that these plants likely

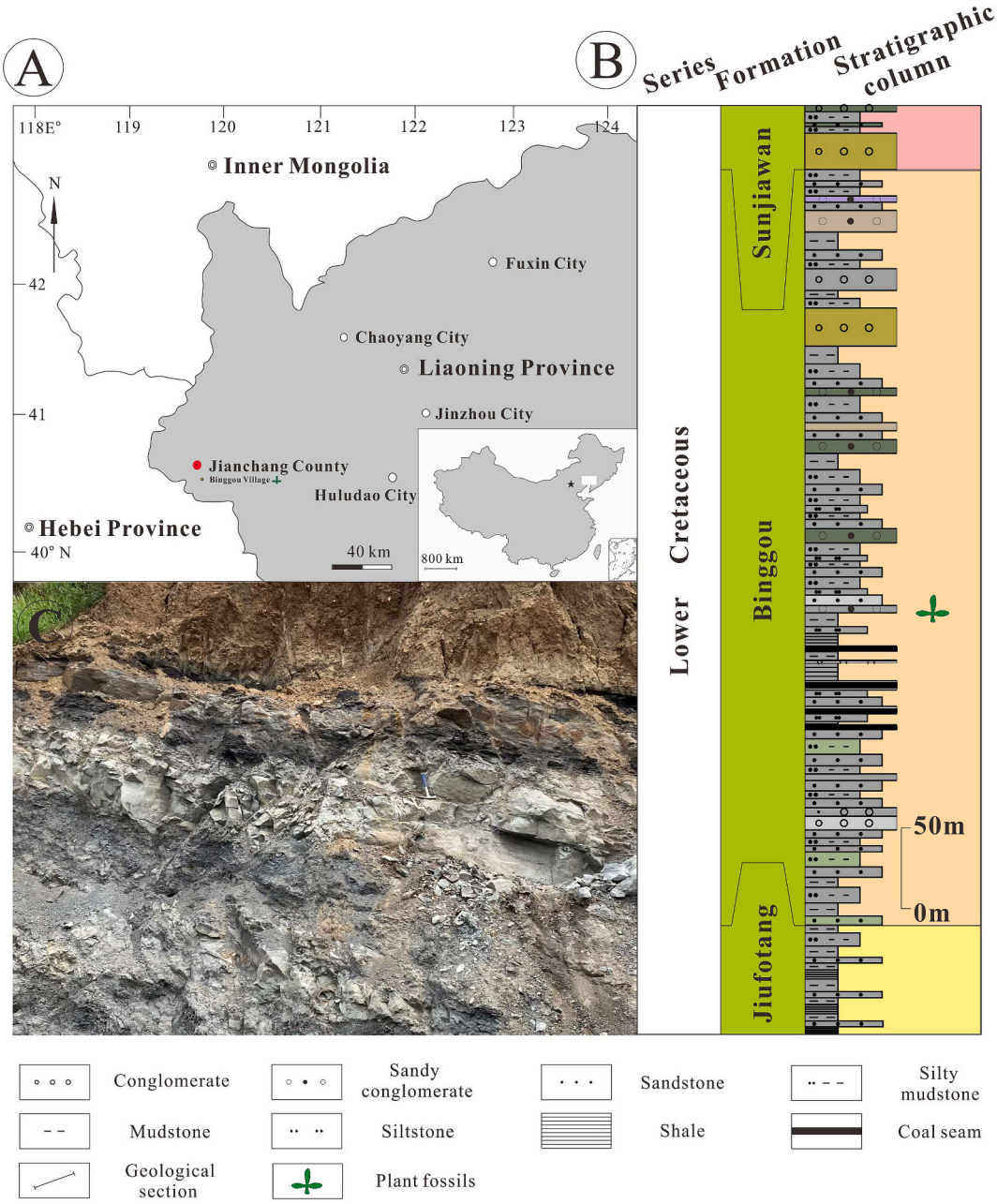

Fig. 1. (A) Location of Jianchang county in Liaoning Province, Northeast China, and the inset image with a leaf symbol indicates the fossil site near Binggou Village. (B) Stratigraphic column of the Lower Cretaceous Binggou Formation near Binggou Village (modified from Tian et al., 2017 and Tan et al., 2026). (C) Photo showing the outcrop.

thrived in warm, frost-free environments (Norstog and Nicholls, 1997; Jones, 1993). Cycads are also typically heliophilous and are commonly associated with open riverbanks and lake margins, or lowland forest ecosystems (Watson and Sincock, 1992). Na et al. (2014) first reported *Nilssoniopteris binggouensis* Na et al. from the Lower Cretaceous Binggou Formation of the Jianchang Basin in Northeast China, representing an easternmost occurrence on the Eurasian continent during this period. We recovered a *Nilssoniopteris* specimen, notable for its exceptionally large leaf (macrophyll) and well-preserved cuticle from the same locality, which is described herein as a new species. In addition, recent studies have refined the stratigraphic age of the Binggou flora to approximately 106.5 ± 1.9 Ma (Tan et al., 2026), placing it within the OAE 1b–c interval of the late Albian and thereby providing a potential climatic context for this disovery. In this paper, we describe the morphology of this new species in detail and, by plotting the occurrences of *Nilssoniopteris* on the Scotese paleogeographic maps, compile and analyze the global spatio-temporal distribution of the genus to elucidate its biogeographic history and paleoclimatic implications.

2. Geological setting, materials and methods

The fossil site is near the Binggou Village (coordinates: 40°47′48″N, 119°50′51″E) in the Jianchang County (Fig. 1a), western Liaoning Province. The study area is situated in the Jianchang Basin, which is within the eastern segment of the Yanshan tectonic belt and represents a faulted basin formed under Mesozoic tectonic activity. The Lower Cretaceous Binggou Formation is well-exposed in this area. The formation, with a total thickness of approximately 485.8 m, is composed primarily of brownish-gray and gray-white conglomerates interbedded with feldspathic sandstones and thin coal seams, representing typical terrestrial deposits. The Binggou Formation lies conformably on the Lower Cretaceous Jiufotang Formation and is conformably overlain by the Sunjiawan Formation.

The Binggou Formation is considered contemporaneous with the upper Shahai and lower Fuxin formations of the Fuxin Basin. Previous biostratigraphic studies suggested a late Early Cretaceous (Aptian–Albian) age for the strata. A recent isotope geochronological study has provided a more precise constraint, yielding an age of 106.5 ± 1.9 Ma (Albian) for the Binggou Formation (Tan et al., 2026). The fossil assemblage, including diverse plants, insects, and conchostracans, indicates a shallow-water-influenced terrestrial ecosystem during the mid–late Early Cretaceous. The palaeovegetation was dominated by gymnosperms (Cycadales, Ginkgoales, Czekanowskiales, and Coniferales) with a minor component of ferns, suggesting a diverse plant community under a predominantly warm and humid paleoclimate that may have experienced seasonal fluctuations (Tan et al., 2026).

The plant fossils described in this study were collected from the middle and lower parts of the Binggou Formation. These strata consist of detrital sandstone, shale, and siltstone with coal seams (Fig. 1b). The fossil specimens and slides were assigned the prefix “PMOL-BG” and are stored at the Paleontological Museum of Liaoning (PMOL), Shenyang, Liaoning Province, China.

Macroscopic photographs were taken using a Canon 5D Mark II digital camera and a Keyence VHX-5000 large depth-of-field microscope. The cuticle material was prepared using standard maceration procedures (Dilcher, 1974; Kerp, 1990; Kerp and Krings, 1999). The prepared cuticles were observed and photographed using a JSM-6700 CF scanning electron microscope at an accelerating voltage of 8 kV.

3. Systematic paleobotany

Order: Bennettitales Engler, 1892

Family: Incertae Sedis.

Genus: ***Nilssoniopteris*** Nathorst, 1909, emend. Cleal et al. (2006).

Type species: *Nilssoniopteris solitaria* (Phillips, 1829) Cleal and Rees, 2003.

Species: *Nilssoniopteris macrophylla* sp. nov. Wang, Tan, Zhang et Sun (Figs. 2–4).

Holotype: PMOL-BG007 (Fig. 2A). This specimen was previously cataloged as RCPS-BGF007–1 because it was temporarily deposited at the Research Center of Paleontology & Stratigraphy at Jilin University, Changchun, Jilin Province, China.

Repository: The Paleontological Museum of Liaoning, Shenyang, Liaoning Province, China.

Type locality: Binggou Village (40°47′56″ N, 119°50′55″ E), Jianchang County, Liaoning Province, China.

Horizon and age: Binggou Formation; late Albian (Early Cretaceous).

Etymology: The specific epithet indicates its large leaf size.

Species diagnosis: Leaf large, thick, linear–lanceolate; middle portion of uniform width (> 10.8 cm), entire-margined leaf; apex obtuse. Rachis slender, smooth; lateral veins parallel, simple, unbranched, dense (18–22 per cm). Upper cuticle astomatic; epidermal cells with strongly sinuous anticlinal walls. Lower cuticle with stomata confined to intercostal bands; stomata brachyparacytic (syndetocheilic), scattered, irregularly oriented, with a density of ca. 40–50 per mm^2. Epidermal cells polygonal in interveinal areas, rectangular along veins; anticlinal walls distinctly sinuous, without ridges; surface smooth with fine grains. Subsidiary cells small, outer walls broad, inner walls typically bulging over guard cells. Guard cells well cutinised; aperture ca. 22 μm long, sunken in a pit often constricted by subsidiary cell ingrowths.

Description: The preserved leaf fragment is approximately 16.5 cm long and 10.8 cm wide. The leaf margin is entire; the apex is obtuse and rounded. The rachis is slender and straight, about 1–2 mm wide. The lamina is laterally attached to the rachis, and the leaf surface bears fine, sparse wrinkles (Fig. 2A–C). The lateral veins are parallel and unbranched, arising from the rachis at 60–70° angles. Vein density is 20 per cm (Fig. 2B, C).

The leaf is hypostomatic. Both the upper and lower epidermis are relatively thin. The outer surface of the upper cuticle is generally smooth (Fig. 3A). On its inner surface, distinct costal bands and intercostal bands are visible. The costal bands, approximately 50 μm wide, consist of 2–3 rows of elongated cells with relatively straight anticlinal walls. The intercostal bands, approximately 500 μm wide, are composed of irregularly shaped cells with strongly sinuous, ring-like anticlinal walls (Fig. 3B, C).

On the inner surface of the lower cuticle, costal bands and intercostal bands are also distinct. The cellular morphology resembles that of the upper cuticle, with sinuous anticlinal walls (Fig. 3D, E, K). The costal bands are about 50 μm wide, and the intercostall bands about 500 μm wide (Fig. 3D). Stomata are confined to the intercostal bands. They are densely and irregularly distributed, with some oriented parallel to the veins (Fig. 3E). The stomata are nearly circular, measuring 40–50 μm in diameter (Fig. 3F–H). The stomata is syndetocheilic. Stomatal density is approximately 45 per mm^2, and the stomatal pore is 2–3 μm wide (Fig. 3J).

Discussion: The current specimen is incompletely preserved, retaining only the middle to upper portion of the leaf. Based on the relatively complete leaves characteristics of the *Nilssoniopteris* that have been published, i.e., *N. angustifolia* (Wang, 1984; Zhao, 2018), *N. angustior* (Pott et al., 2007), *N. longifolius* (Chang, 1976; Wang et al., 2022), *N. changcaiensis* (Li, 2017). The average length-to-width ratio is about (3.6–11.1):1. It is speculated that, the estimated total leaf length of the new specimen might be no less than 30 cm.

Remarks and comparisons: The present specimen shows the characteristics of *Nilssoniopteris*, including entire-margined leaves with taeniopteroid venation, a hypostomatic epidermis with rectangular to polygonal epidermal cells bearing sinuous anticlinal walls, and syndetocheilic stomata confined to the abaxial surface. These features are fully consistent with the diagnosis of *Nilssoniopteris*. Therefore, it is reasonable to assign the present material to this genus.

The new species is compared with *Nilssoniopteris bolei* Barale from the Middle Jurassic of Henan (Barale et al., 1998), *N. beyrichii* (Schenk)

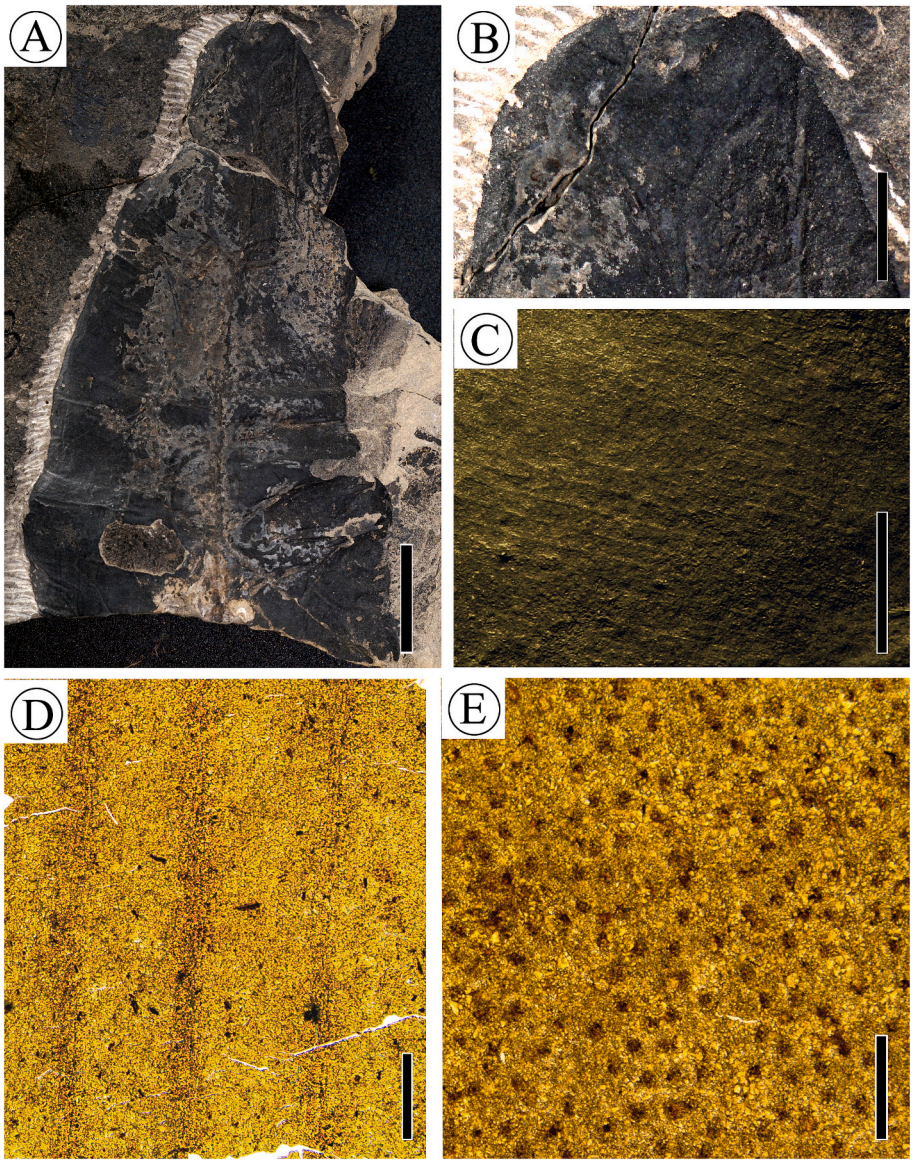

Fig. 2. *Nilssoniopteris macrophylla* sp. nov. (RCPS-BGF007–1). (A–B) Images showing frond morphology. (C) Enlargement of (A) showing venation. (D) Upper cuticle showing the costal and intercostal zones. (E) Lower cuticle showing a costal zone, an intercostal zone, and stomata.
Scale bars: A = 30 mm, B = 15 mm, C = 4 mm, D = 250 μm, E = 300 μm.

Nathorst from the Early Cretaceous of the Huolinhe Basin (Deng, 1995), *N. prynadae* Samylina (Deng, 1995), *N. multiformis* Deng (Deng, 1995), and *N. binggouensis* Na et al. from the same formation in the Jianchang Basin (Na et al., 2014) (Table 1).

Among these, the new specimen is most similar in overall leaf shape to *N. bolei* and *N. multiformis*. However, it differs from them in several respects. *N. bolei* has forked veins and stomata arranged in a regular, oriented pattern, while the currunt specimen has unforked veins and stomata arrangement irregular; *N. multiformis* exhibits a wide range of pinnule shapes (strap-shaped to oval), possesses transverse striations on the rachis, has a lower vein density (18 per cm), and its stomata are arranged in three rows and are nearly square or elliptical, while the current specimen displays a consistently linear leaf shape, has a higher vein density, and its stomata are not arranged in distinct rows, but are densely and irregularly scattered across the intercostal bands.

The new species differs from other species as follows: *N. beyrichii* is much smaller than the present specimen, and its veins are usually branched once, unlike the parallel and unbranched veins of the current specimen. *N. prynadae* has strap-shaped leaves with nearly parallel sides, fine transverse striations on the rachis, partially forked veins, and square or rhombic stomata arranged in bands with slits oriented perpendicular, parallel, or oblique to the veins. In contrast, our specimen lacks transverse striations, has strictly unbranched veins, and its stomata are irregularly oriented. *N. binggouensis*, although from the same stratum (the Binggou Formation) as our specimen, differs significantly in both pinnule morphology and epidermal structure. The most significant difference between them is that the former has an acute apex, while the latter possesses an obtuse and rounded apex. Other species listed in Table 1 (e.g., *N. ciniza* Ash, *N. musafolia* Barnard, *N. neimenguensis* (Wang, 1984) Zhao et Deng, *N. zirabensis* Schweitzer et Kirchner, *N. inconstans* Sun et Shen, *N. pristis* Harris, *N. hamiensis* Zhao et Deng, *N. pannuceus* Bose et Banerji, *N. hailarensis* Zheng et Zhang, *N. oishii* Yamada, Nishida et Legrand, *N. platyrachis* (Samylina) Sun et Li, *N. changcaiensis* Sun et Li, *N. tomentosa* Herrera et al., *N. shiveeovoensis* Herrera et al., and *N. pecinovensis* J. Kvaček) differ from our specimen in having smaller leaf size, lower or higher vein density, forked veins, distinctly different stomatal orientation, or other combinations of characters, and thus are distinct from the present species.

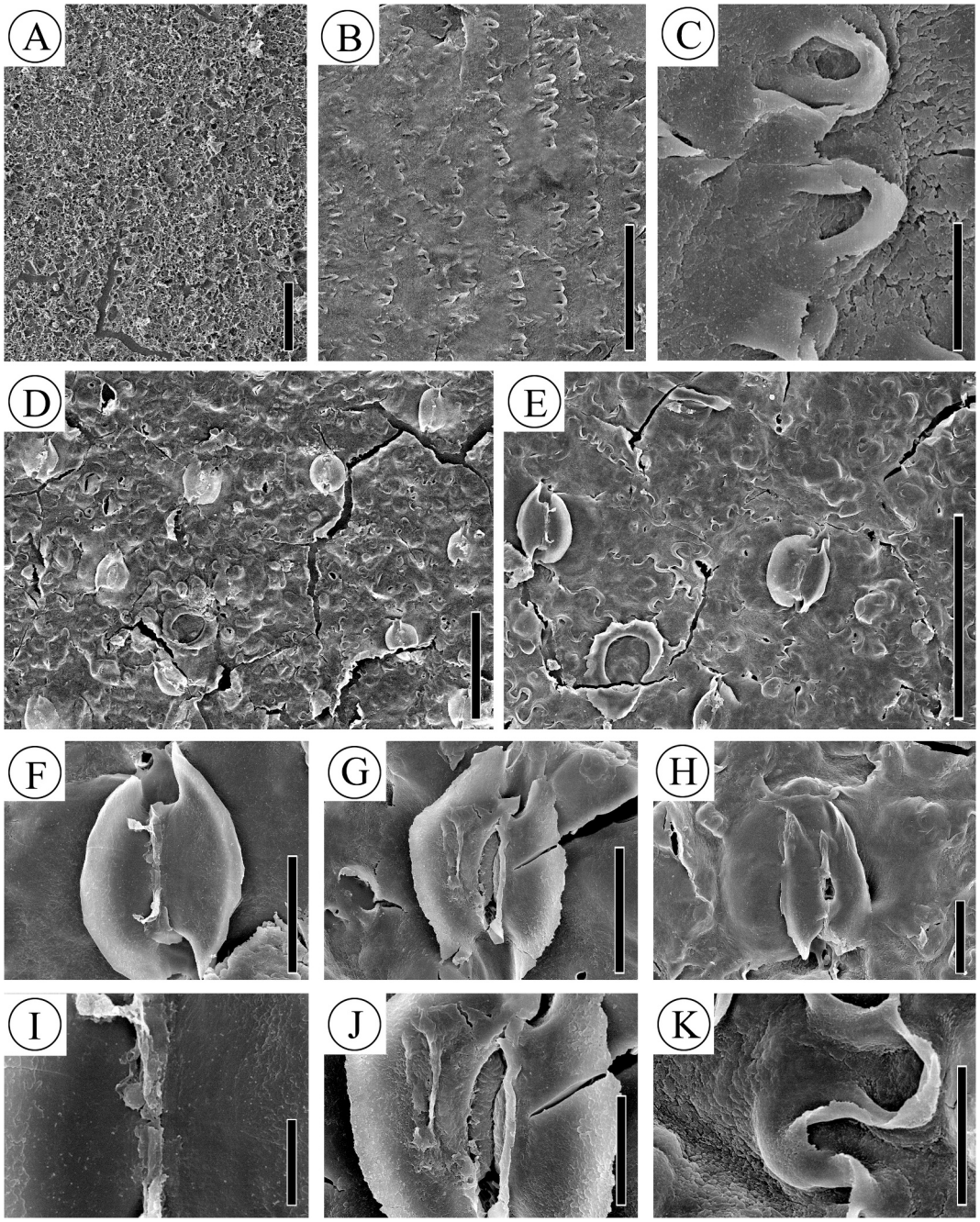

Fig. 3. Cuticular micromorphology of *Nilssoniopteris macrophylla* sp. nov. (A) Relatively smooth outer surface of the cuticle, showing no distinct features to differentiate the upper and lower cuticles. (B–C) Inner surfaces of the upper cuticle. B shows the polygonal epidermal cells on the inner surface of the upper cuticle, and C shows the enlargement of the sinuous area in (B). (D–K) Inner surface of the lower cuticle. D and E show the arrangement of the stomatal apparatuses; F–H show closed, open, and partially closed stomatal apparatuses, respectively; I and J show enlargements of the stomatal apparatuses in (F) and (G), respectively; K shows the epidermal anticlinal walls, which exhibit a distinctive S-shaped pattern due to strong sinuation.
Scale bars: A = 20 μm, B = 50 μm, C = 20 μm, D = 100 μm, E = 100 μm, F–H = 20 μm, I–K = 10 μm.

In conclusion, the new species differs from all other known species in the following combination of features: obtuse leaf apex; lamina width tapering apically; rachis with fine longitudinal striations; veins unbranched and dense (18–22 per cm); stomata nearly circular, densely and irregularly scattered across the intercostal bands; and epidermal cells with strongly sinuous anticlinal walls.

4. Spatio-temporal distribution and paleoclimatic implications

The exceptionally large leaf and well-preserved cuticle of *Nilssoniopteris macrophylla* offer an opportunity to explore the relationship between leaf morphology and paleoclimate. However, to fully assess the climatic significance of this new species, it is necessary to place it within the broader context of the global distribution of *Nilssoniopteris* through time.

4.1. Large leaf size as an indicator of humid climate

The most striking feature of the new specimen is its exceptionally broad and large leaf. Although only the middle and upper portions are

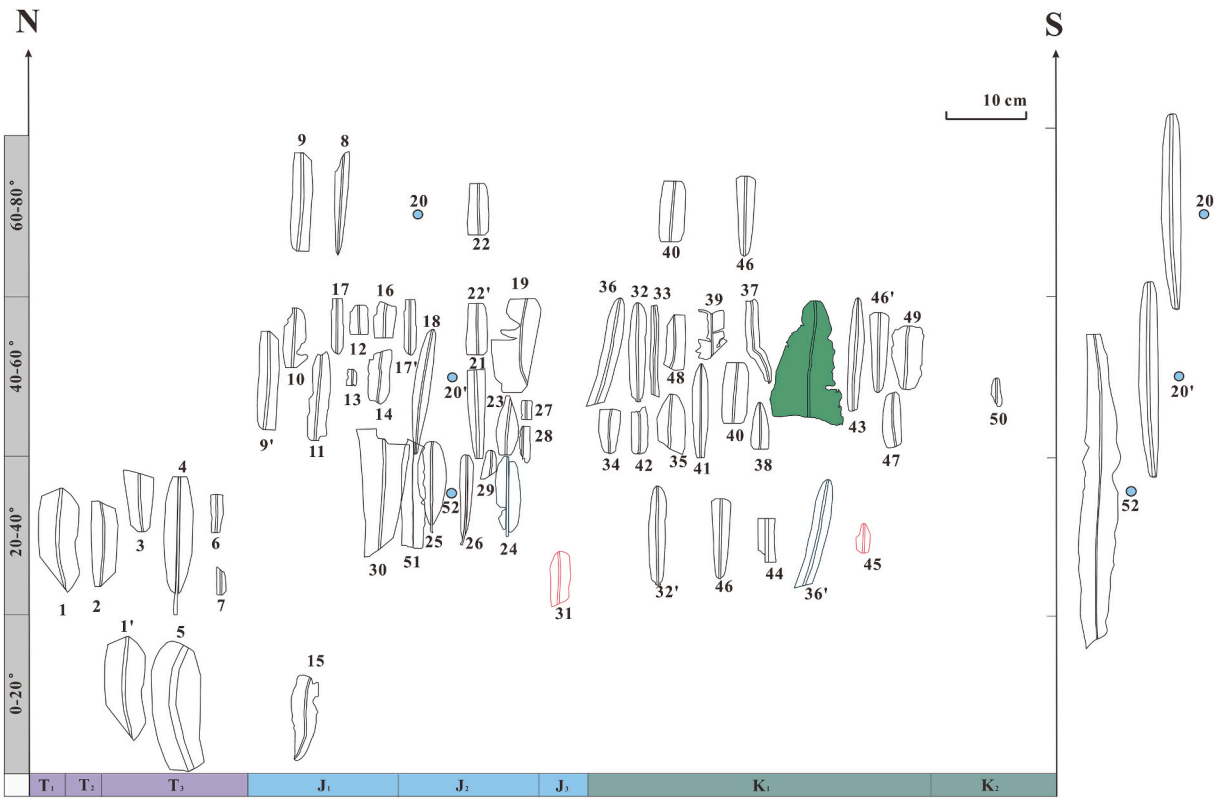

Fig. 4. Line drawings showing distribution of *Nilssoniopteris* in the Mesozoic in different paleo–latitude phase.
Note: the line drawings are based on the records with pictures (totally 52 leaves, listed below). The horizontal axis is segmented into the Triassic, Jurassic, and Cretaceous periods; however, due to layout constraints, further subdivisions have not been included. The vertical axis denotes paleo–latitude; The central point of each leaf line graph is positioned on the corresponding latitude band, with minor adjustments made for optimal layout arrangement.
1. *N. jourdyi* (Li et al., 1976; Yang, 1978; Xu et al., 1979; Wang, 1993); 2. *N. immersa* (Li et al., 1976); 3. *N. tenuinervis* (Li et al., 1976); 4. *N. angustior* (Pott et al., 2007); 5. *N. ciniza* (Ash, 1978); 6. *N. oligotricha* (Zhou, 1989); 7. *N. xuiana* (Zhou, 1989); 8. *N. neimenguensis* (Wang, 1984; Zhao, 2018); 9. *N. glandulosa* (Kiritchkova and Nosova, 2012); 10. *N. papillifera* (Kiritchkova and Nosova, 2012); 11. *N. artemii* (Kiritchkova and Nosova, 2012); 12. *N. denticaligera* (Kiritchkova and Nosova, 2012); 13. *N. kokalensis* (Kiritchkova and Nosova, 2012); 14. *N. zinea* (Kiritchkova and Nosova, 2012); 15. *N. intermedia* (Sohweitzer et al., 2003); 16. *N. iocalis* (Kiritchkova and Nosova, 2012); 17. *N. linearis* (Kiritchkova and Nosova, 2012); 18. *N. angustifolia* (Doludenko and Svanidze, 1969; Wang, 1984); 19. *N. inconstans* (Sun et al., 1988); 20. *N. longifolius* (Zhang, 1984; Wei et al., 2005); 21. *N. pristis* (Harris, 1969; Li et al., 1988); 22. *N. vittata* (Si, 1963; Harris, 1969; Chen et al., 1984; Wang, 1984); 23. *N. bolei* (Barale et al., 1998); 24. *N. major* (Harris, 1969); 25. *N. hamiensis* (Zhao, 2018); 26. *N. solitaria* (Pott and Van Konijnenburg-van Cittert, 2017); 27. *N. infera* (Gordenko, 2008); 28. *N. saveljevii* (Kiritchkova and Nosova, 2012); 29. *N. chirchilica* (Kiritchkova and Nosova, 2012); 30. N. *crassiaxis* (Zhao, 2018); 31. *N. pannuceus* (Bose et al., 1984); 32. *N. beyrichii* (Wang, 1984; Chen et al., 1988; Deng, 1995); 33. *N. hailarensis* (Zheng et al., 1990); 34. *N. multiformis* (Deng, 1995); 35. *N. ovalis* (Deng, 1995; Chen et al., 1988); 36. *N. prynadae* (Samylina, 1964; Chen et al., 1988; Deng, 1995; Wei et al., 2005); 37. *N. binggouensis* (Na et al., 2014); 38. *N.* sp. (Wei et al., 2005); 39. *N. oishii* (Yamada et al., 2009); 40. *N. platyrachis* (Samylina, 1976; Wei et al., 2005); 41. *N. changcaiensis* (Li, 2017); 42. *N. tomentosa* (Herrera et al., 2018); 43. *N. shiveeovoensis* (Herrera et al., 2018); 44. *N. corrugata* (Ray et al., 2014); 45. *N. variabilis* (Bose et al., 1984); 46. *N. rhitidorachis* (Oishi, 1935; Samylina, 1961; Samylina, 1963; Krassilov, 1967); 47. *N. didaoensis* (Chen et al., 1988); 48. *N.* sp. (Chen et al., 1988); 49. *N. arctica* (Seward, 1927; Boyd, 2000); 50. *N. pecinovensis* (Kvaček, 1995); 51. *N. baojishanensis* (Zhang et al., 2026); 52. *N. specialis* (Zhang et al., 2026)

preserved, a reconstruction based on comparison with complete *Nilssoniopteris* leaves suggests that the total leaf length is estimated to be no less than 30 cm (see Chapter 3, Discussion). This size is exceptional among known *Nilssoniopteris* species (Fig. 4), although some deeply lobed bennettitalean leaves (e.g., *Ctenis*) could reach or exceed this length.

According to global plant ecophysiological studies, leaf size is primarily constrained by water availability: large-leaved species predominate in humid environments with ample warmth and sunlight, whereas in arid regions, leaves are typically small regardless of temperature (Peppe et al., 2011; Wright et al., 2017; Baird et al., 2021). The large leaf of *N. macrophylla* therefore points to a warm–hot, moisture-sufficient (humid–mesic) environment in which water supply is adequate to support transpirational cooling of a large lamina without imposing water stress.

The principle of uniformitarianism provides additional insight (Little et al., 2010). Extant cycads are generally regarded as the nearest living relatives of Bennettitales, and those species with broad leaves among them are typically found in warm environments free of frost and with abundant moisture. For instance, *Ceratozamia euryphyllidia* from Mexico produces exceptionally broad leaflets, up to 16 cm in width, and grows in wet tropical evergreen rainforests at low elevations (Vázquez Torres et al., 1986; Jones, 1993). Similarly, *Zamia amplifolia* from northwestern Colombia is characterized by strikingly large leaves and inhabits tropical rainforests with consistently high humidity (Masters, 1878). In Africa, *Encephalartos latifrons*, a species whose specific epithet refers to its broad fronds, bears leaflets up to 6.2 cm wide and occurs in scrub bush on rocky hill slopes within a subtropical climate (Palmer and Pitman, 1972). This convergence in leaf morphology among distantly related cycad lineages suggests that broad leaflets confer a functional advantage under warm, humid, and frost-free conditions, thereby providing a comparative framework for interpreting the large leaves with entire margins observed in *N. macrophylla.*

The extant monocot *Strelitzia reginae*, which, despite its distant phylogenetic relationship to Bennettitales, shows a strong morphological convergence with *N. macrophylla* in having large, entire, coriaceous leaves, occurs naturally along the eastern coast of South Africa in coastal bush, thicket, and along river banks, within a warm, frost-free

Table 1
A comparative of morphological characteristics of the genus *Nilssoniopteris*.

Species	Leaf morphological characteristics								Stomata characteristics				Location epoch	References
	Lamina shape	Lamina size (L x W cm)	Rachis width (mm)	Axial surface ornamentation	Lateral vein branching	Veins per cm	Lamina margin	Trichome	Stomatal type	Stomata density	Stomatal distribution	Stomata orientation		
Nilssoniopteris macrophylla sp. nov.	–	21 ~ 22 × 9 ~ 10	1 ~ 2	Fine longitudinal striations	Simple	18 ~ 22	Entire	–	Syndetochelic	45	Dense	Parallel circuit	Jianchang, Liaoning, K_1	This paper
N. ciniza	Linear–lanceolate	20 ~ 30 × 7 ~ 10	1 ~ 5	Cross striation	Simple	35 ~ 60	Entire	–	Syndetochelic	0 ~ 5/40 ~ 50/60 ~ 80	Parallel distribution	Vertical circuit	North America, T_3	Ash (1978)
N. musafolia	Oval to lanceolate	>22 × 6 ~ 12	8	Smooth/ Fine longitudinal striations	Forked once or twice	6 ~ 26	Entire	Present	–	50 ~ 60	–	Vertical circuit	Iran, T_3 Iran, J_1	Schweitzer and Kirchner (2003) Barnard (1965)
N. neimenguensis	Linear / Strap shaped	>8 × 0.9 ~ 1.3	0.7 ~ 1–	–	Simple or forked once	15 ~ 21	Entire	Present	Syndetochelic	–	–	Irregularly distributed	Xilinhot, Neimenggu, J_1	Zhao (2018); Wang (1984)
N. zirabensis	Long elliptic to lanceolate	>16 × 2 ~ 2.5	1.5 ~ 3	longitudinal grain / Cross striation	Simple or forked once	22 ~ 26	Entire	Absent	–	57	Stomatal band	Irregularly distributed	Iran, J_1	Schweitzer and Kirchner (2003)
N. inconstans	Strap shaped	11.5 × 8.5	3	Smooth / Longitudinal grain	Forked once	18 ~ 20	Lower part is entire; upper part is pinnately divided	Present	Syndetochelic	60 ~ 80	Dense	Randomly oriented	Lanzhou, Gansu, J_2	Sun and Shen (1988)
N. pristis	Long strap shaped, Linear	12 x (2.5 ~ 4)/ 1 ~ 3(W)	Base: 4 ~ 5 Middle: 3 ~ 4 Top: 1 ~ 2	Cross striation	Simple or forked once	15 ~ 25	Entire	Present	Syndetochelic	–	–	Oriented	Chaidamu, Qinghai, Yorkshire, England, J_2	Li et al. (1988); Harris (1969)
N. hamiensis	Narrowly elliptical to Oblanceolate	17 x (4 ~ 6/2.5 ~ 4)	2 ~ 3	–	Simple, forked once or twice	16 ~ 34	Entire	Present	Syndetochelic	25 ~ 55	–	Randomly oriented	Xinjiang, J_2	Zhao (2018)
N. pannuceus	linear to lanceolate	>13.4 × 2.8	2 ~ 2.8	Longitudinal grain	Simple or furcation	12 ~ 20	Entire	Present	–	50	–	Vertical circuit, minority Parallel circuit	India, J_3	Bose and Banerji (1984)
N. beyrichii	Strap shaped	1.2 ~ 2.5 (W)	2	Cross striation	Forked once	20	Entire	Absent	–	–	Unevenness	Randomly oriented	Huolinhe, Neimenggu, Hebei, Liaoning, K_1	Deng (1995); Wang (1984); Chen et al. (1988)
N. hailarensis	Narrowly linear	8 x (0.5 ~ 0.6)	1 ~ 3	–	Simple or forked once	16 ~ 20	Entire	Present	Syndetochelic	20 ~ 25	Loose	Heterotropic or vertical circuit	Hailaer, Neimenggu, K_1	Zheng et al. (1990)

(*continued on next page*)

Table 1 (*continued*)

Species	Leaf morphological characteristics								Stomata characteristics				Location epoch	References
	Lamina shape	Lamina size (L x W cm)	Rachis width (mm)	Axial surface ornamentation	Lateral vein branching	Veins per cm	Lamina margin	Trichome	Stomatal type	Stomata density	Stomatal distribution	Stomata orientation		
N. multiformis	Strap shaped to Oval	Strap shaped:12 x (2.2 ~ 5) Ova:2.2 × 1.5	1 ~ 2	Cross striation	Simple or forked once	18	Entire	Present	Syndetochelic	70 ~ 80, stomatal band 100	Triplex row	–	Huolinhe, Neimenggu, K_1	Deng (1995)
N. prynadae	Strap shaped	10 × 3.2	1.5 ~ 2.5	Fine cross striation	Forked once	20	–	Present	Syndetochelic	–	Stomatal band	Heterotropic, parallel or vertical circuit	Huolinhe, Neimenggu, Liaoning, Jilin, Russia, K_1	Deng (1995); Chen et al. (1988); Samylina (1964); Wei et al. (2005)
N. binggouensis	Strap shaped	14 x (1–1.3)	0.8 ~ 1.2	Smooth	Forked once	20 ~ 30	Entire	Absent	Syndetochelic	45 ~ 65	Irregularity	Vertical circuit	Jianchang, Liaoning, K_1	Na et al. (2014)
N. oishii	Strap shaped	1.8 × 0.9	2.8	–	Simple	27 ~ 30	Segmented	Present	Syndetochelic	–	Directional alignment	Vertical circuit	Southwestern Japan, K_1	Yamada et al. (2009)
N. platyrachis	Strap shaped	8 × 3.4	2 ~ 3	–	Simple or forked once	10 ~ 11	Entire	Absent	Syndetochelic	50 ~ 70	Irregularity	–	Magadan, Russia, Jilin, K_1	Samylina (1976); Wei et al. (2005)
N. changcaiensis	Long strap shaped	22 × 2.2	1	–	Simple	30	Entire	–	Syndetochelic	25 ~ 35	Unevenness	Randomly oriented	Yanbian, Jilin, K_1	Li (2017)
N. tomentosa	Strap shaped	1.25 ~ 2.8 (L)	2 ~ 4.3	Cross striation	Simple, forked twice	30 ~ 80	Entire	Present	Syndetochelic	65 ~ 82	–	Vertical circuit	Mongolia, K_1	Herrera et al. (2018)
N. shiveeovoensis	Strap shaped	(15 ~ 19) x (1.4 ~ 2.0)	1.5 ~ 3.5	Cross striation to smooth	Simple, forked twice	25 ~ 50	Entire	Present	Syndetochelic	36 ~ 50	–	Heterotropic, parallel or vertical circuit	Mongolia, K_1	Herrera et al. (2018)
N. pecinovensis	Linear	1 × 0.35	–	–	Simple or forked once	18 ~ 20	Entire	Present	Syndetochelic	–	Parallel distribution	Vertical circuit	Czechia, K_2	Kvaček (1995)
N. bolei	Obovate - lanceolate	(10 ~ 15) x (1.0 ~ 2.3)	–	Flat and smooth	Simple or forked once	12 ~ 24	Entire	Present	Syndetochelic	–	Irregularity	Irregularly distributed	Henan, J_2	Barale et al. (1998)

Note: Abbreviations for geological ages follow the standard Chinese geological time scale: T_3 = Late Triassic; J_1 = Early Jurassic; J_2 = Middle Jurassic; J_3 = Late Jurassic; K_1 = Early Cretaceous; K_2 = Late Cretaceous.

subtropical climate (SANBI [South African National Biodiversity Institute], PlantZAfrica.com; Missouri Botanical Garden). This ecological preference suggests that large, entire-margined leaves in *N. macrophylla* may reflect adaptation to analogous conditions—namely, a warm, frost-free, and humid climate, rather than a cool or arid one.

In summary, the large leaf size of *N. macrophylla* provides compelling evidence for high humidity in the Jianchang Basin during the Albian, and the ecological preference of morphologically analogous modern plants suggests that this humidity was accompanied by frost-free (and likely warm) conditions.

4.2. Entire leaf margin as an indicator of warm climate

In addition to leaf size, leaf margin analysis provides independent paleoclimatic evidence. Entire (smooth, non-toothed) margins in dicotyledonous plants show a well-established positive correlation with mean annual temperature, a pattern first documented by Bailey and Sinnott (1915, 1916) and later formalized as leaf margin analysis (Wolfe, 1995). This relationship has been validated in modern Chinese flora (Chen et al., 2019) and consistently applied to Cenozoic palaeotemperature reconstructions (Dai et al., 2023).

Globally, entire-margined leaves usually predominate in perennially warm, frost-free tropical and subtropical regions. From a physiological perspective, entire margins are advantageous in relatively stable warm environments because they avoid the increased frost damage risk associated with toothed margins under cold conditions and reduce water loss under drought stress (Givnish, 1987; Lambers et al., 2008). Based on this inference, the entire margin of *N. macrophylla* is therefore consistent with adaptation to a warm palaeoclimate.

Although leaf margin analysis is most robust when applied to entire fossil floras rather than single species, the presence of an entire-margined leaf in *N. macrophylla*—coupled with its large size (Section 4.1)—adds to another line of evidence for a warm and humid Albian climate in NE China.

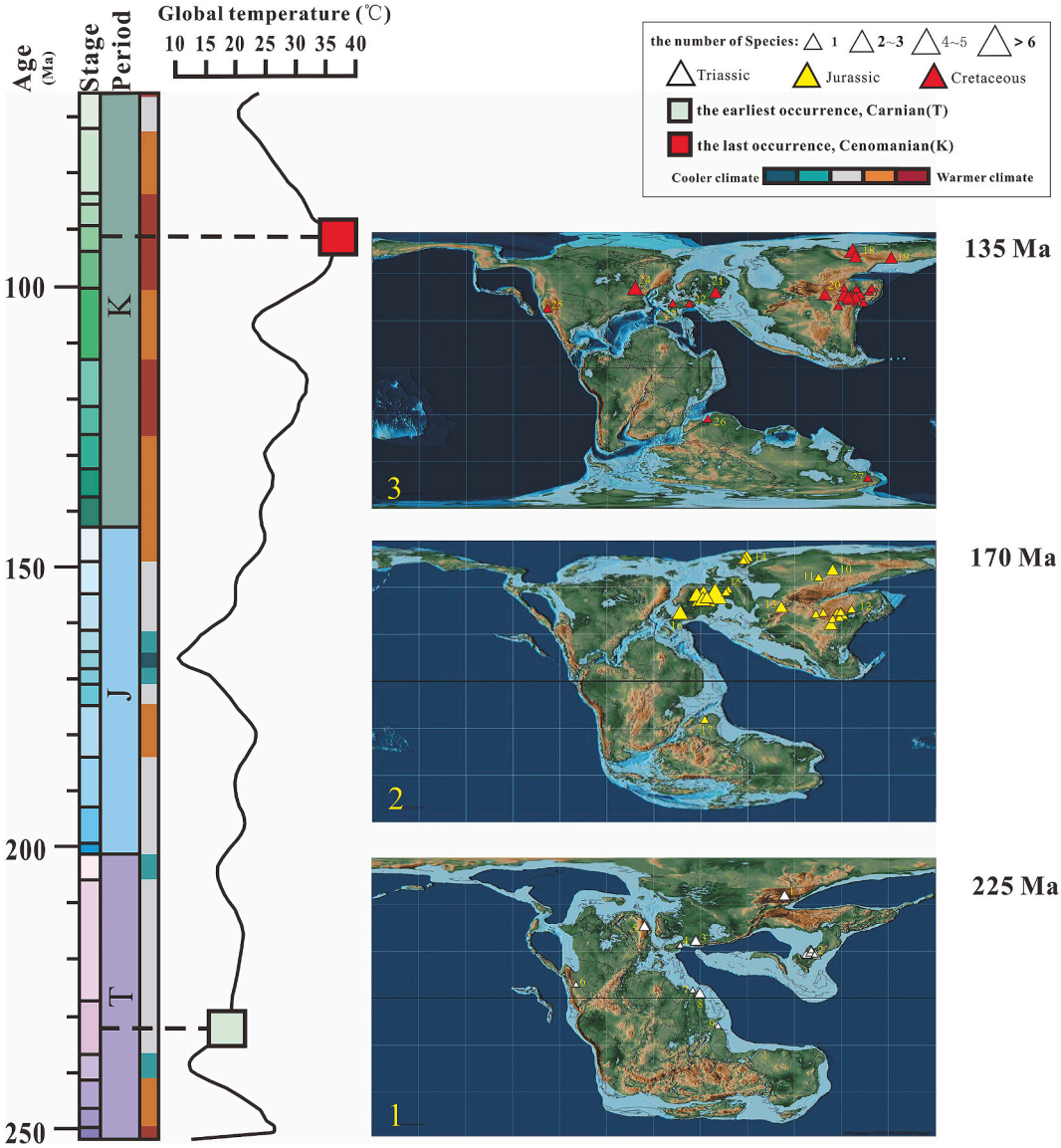

Fig. 5. Expansion of *Nilssoniopteris* into higher latitudes plotted on paleogergraphyic map from the Triassic to the Early Cretaceous. Paleogeographic coordinates were calculated using the Paleolocation Mapping Service (PAMS) available at paleolocation.org (Urban and Hardisty, 2013). Colors of triangular symbols indicate fossil occurrence sites of different periods.

4.3. Northward migration of Nilssoniopteris as revealed by global fossil records

Our compilation of 93 global fossil occurrences demonstrates an obvious paleobiogeographic trend: *Nilssoniopteris* progressively expanded its distribution northward from the Late Triassic to the Cretaceous (Fig. 5). This pattern aligns with the genus' inferred preference for warm and humid climates.

Late Triassic (low-latitude origin). The genus first appeared in the Carnian, with records from Austria (Pott et al., 2007) and southern China. All occurrences were confined to low-latitude tropical–subtropical humid zones of the Pangaea (Fig. 5), indicating a strict thermophilic and hygrophilic preference.

Jurassic (mid-latitude expansion). During the Jurassic, *Nilssoniopteris* reached its peak diversity and expanded into mid-latitudes of the Laurasia (e.g., China, Iran, UK). However, its absence from high latitudes suggests that climatic thresholds – particularly low temperatures – still limited its distribution.

Cretaceous (northward shift). The Early Cretaceous witnessed an obvious northward migration. Occurrences in NE China (Hebei, Liaoning, Jilin), the Russian Far East, Mongolia, and Canada (Vancouver Island) suggest the presence of this genus at higher paleolatitudes than ever before (Fig. 5). This expansion coincided with the intense greenhouse warming of the Early Cretaceous, which reduced latitudinal temperature gradients and allowed thermophilic plants to extend their ranges poleward.

The new species *N. macrophylla* from the Albian of the Jianchang Basin (NE China) is a critical piece of this evidence. Its exceptionally large leaf and entire margin (Sections 4.1–4.2) are morphological adaptations consistent with a warm, humid greenhouse climate. Its occurrence at mid-high paleolatitude (~42°N) during the Albian directly demonstrates that *Nilssoniopteris* had successfully migrated northward in response to global warming.

The progressive poleward expansion of *Nilssoniopteris* is further quantified in Fig. 6, which plots the paleolatitudinal distribution of all compiled fossil occurrences through geological time. The thick black line in Fig. 6 represents the moving average of the median paleolatitude, clearly illustrating a sustained northward shift from the Triassic to the Cretaceous. This figure thus provides a visual summary of latitudinal migration the genus, complementing the geographic map (Fig. 5) and reinforcing the conclusion that *Nilssoniopteris* responded to Early Cretaceous greenhouse warming by expanding into higher latitudes.

Several global mechanisms likely facilitated this northward expansion. These include a reduced latitudinal temperature gradient during the mid-Cretaceous greenhouse (i.e., warmer conditions at higher latitudes; Huber et al., 2002; Spicer and Herman, 2010), intensified monsoon circulation in East Asia (bringing more moisture to interior regions; Herman and Spicer, 2010; Farnsworth et al., 2019), and changes in Cretaceous seaway configuration that created humid migration corridors along continental margins (Hay, 2008; Sellwood and Valdes, 2006). Collectively, these factors elevated regional temperature and humidity, particularly at middle to high latitudes. Such climatic shifts would have created more hospitable conditions there, thereby reducing environmental constraints—such as cold temperatures and aridity—that previously limited the distribution of thermophilic plants. Consequently, a warm-adapted plant like *Nilssoniopteris* was able to extend its range into middle to high latitudes during the OAE 1b–c interval.

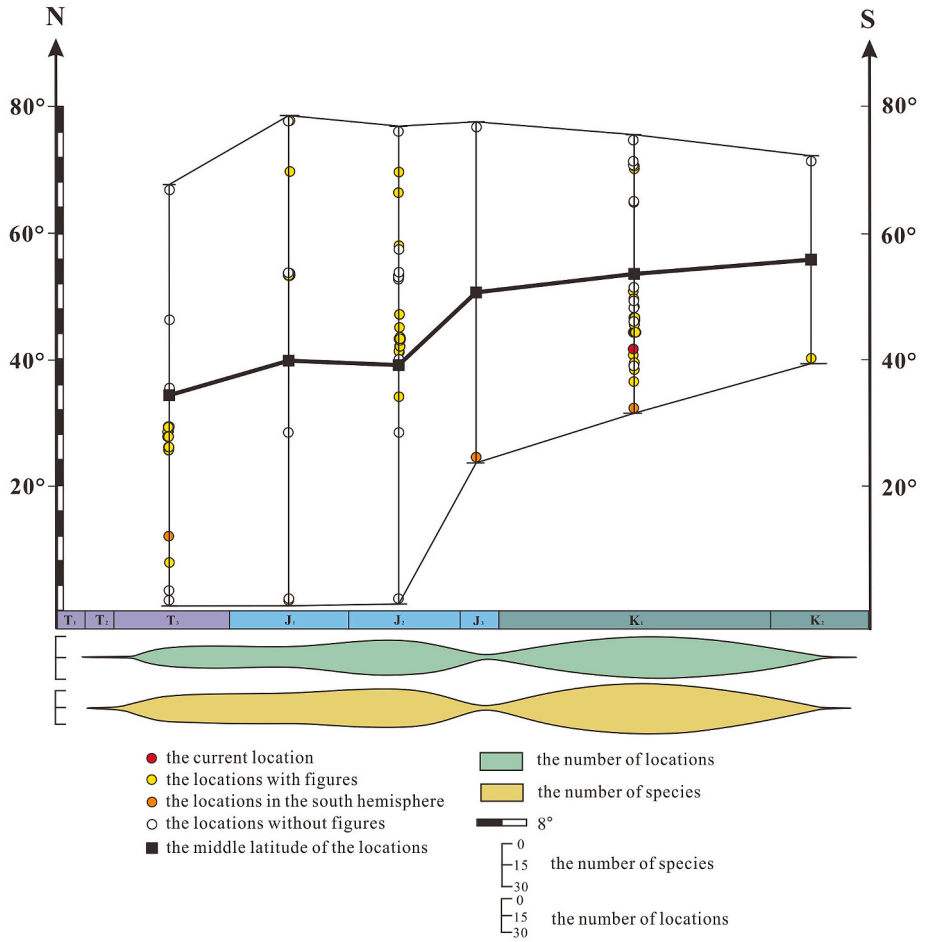

Fig. 6. Spatiotemporal distribution and diversity of *Nilssoniopteris* from the Triassic to the Early Cretaceous.

4.4. Occurrence of *N. macrophylla* during the OAE 1b–c interval: A terrestrial signature of greenhouse warming

The Binggou Formation, which yields *N. macrophylla*, has been dated to 106.5 ± 1.9 Ma (Tan et al., 2026), placing it within the late Albian. This age falls between Oceanic Anoxic Events OAE 1b and OAE 1c—a prolonged interval of global greenhouse warming and disrupted ocean chemistry (Jenkyns, 2010). While OAE 1b and OAE 1c are less intensively studied than OAE 1a or OAE 2, they nevertheless represent significant warm pulses within the mid-Cretaceous thermal maximum.

The presence of *N. macrophylla*—a large-leaved, entire-margined, hypostomatic plant adapted to warm and humid conditions—in the Jianchang Basin at this specific time is unlikely to be coincidental. It suggests that the Albian warming associated with OAE 1b–c had a measurable impact on terrestrial vegetation in NE China, enabling a thermophilic element like *Nilssoniopteris* to thrive at mid-high latitudes.

Other paleontological evidence from the same section (the Binggou Formation) has also provided constraints on the paleoclimate of this area. Palynological data from the Binggou Formation yield a sporopollen assemblage dominated by *Cicatricosisporites-Osmundacidites-Concentrisporites*. The SEG (Sporomorph EcoGroup) model, together with EPH (Effect of Plant Humidity) and EPT (Effect of Plant Temperature) models indices, consistently indicates a stable and humid environment without large scale climatic disturbances (Tan et al., 2026). The xerophytic indicator *Classopollis* accounts for less than 0.5%, further ruling out arid conditions.

Macrofloral remains from the same horizons include *Equisetites*, diverse ferns (*Coniopteris*), abundant bennettitaleans (*Nilssoniopteris*, *Pterophyllum*), ginkgophytes and conifers, all pointing to a warm and humid climate, though without reaching the peak of extreme warmth and humidity (Tan, 2018). The occurrence of hygrophilous elements such as *Equisetites* and *Coniopteris* reinforces this interpretation.

In terms of freshwater fauna, the bivalve assemblage *Ferganoconcha liaoxiensis-Sphaerium anderssoni*, together with diverse conchostracans and ostracods, indicates persistent lacustrine-fluvial conditions with ample water supply (Tian et al., 2017). These independent lines of evidence cross-validate the paleoenvironmental interpretation derived from the present megafossil specimens.

Therefore, two lines of evidence support this interpretation. First, the northward migration documented in Section 4.3 shows that *Nilssoniopteris* reached its highest paleolatitudes during the Cretaceous, and the Jianchang occurrence is part of that trend. Second, the morphological adaptations of *N. macrophylla* (large leaf, entire margin, thick cuticle) are precisely those that would be favored under elevated temperatures and high humidity – conditions expected during OAE 1b–c.

Thus, *N. macrophylla* can be regarded as one of the regional terrestrial indicators for the greenhouse climate of the late Albian, and its occurrence in NE China provides direct fossil evidence that the warming associated with OAE 1b–c extended to mid-high latitude continental settings.

5. Conclusions

(1) A new species, *Nilssoniopteris macrophylla* sp. nov. is described from the Lower Cretaceous Binggou Formation (Albian, 106.5 ± 1.9 Ma) of the Jianchang Basin, NE China. It represents one of the largest known leaves of the genus, and exhibits a well-preserved cuticle with syndetocheilic stomata.

(2) The leaf traits of *N. macrophylla*, including gigantic size, entire margin, thick cuticle, and hypostomatic organization, suggest adaptation to a warm, frost-free, and humid climate.

(3) A global compilation of *Nilssoniopteris* fossil records reveals a northward migration from the Triassic to the Cretaceous. The genus reached its highest paleolatitudes during the Early Cretaceous, with *N. macrophylla* occurring at ~42°N in the Albian. This expansion coincided with the intense greenhouse warming of the mid-Cretaceous.

(4) The age of the Binggou Formation (106.5 ± 1.9 Ma) falls within the OAE 1b–c interval. The occurrence of *N. macrophylla* at this time and location may provide new evidence that the warming associated with these oceanic anoxic events also affected terrestrial vegetation in mid-high latitude continental settings, enabling thermophilic plants to extend their ranges poleward.

In summary, this report not only adds a remarkable new species to the Bennettitales but also demonstrates how integrated morphological and biogeographic analysis of fossil plants can illuminate the adaptation of land plants to Cretaceous greenhouse climates.

Declaration of competing interest

The authors declare the following financial interests/personal relationships which may be considered as potential competing interests: Xiao Tan reports financial support was provided by National Natural Science Foundation of China (No. U2544204). Xiao Tan reports financial support was provided by National Natural Science Foundation of China (No. 41902009). Xiao Tan reports financial support was provided by Liaoning Provincial Department of Education Research Platform Development Project (No. LJ232510166001). Reports a relationship with that includes:. Has patent pending to. If there are other authors, they declare that they have no known competing financial interests or personal relationships that could have appeared to influence the work reported in this paper.

Acknowledgments

This research was jointly supported by the National Natural Science Foundation of China (Grant Nos. U2544204, 41902009), Liaoning Provincial Department of Education Research Platform Development Project (LJ232510166001), Liaoning Science and Technology Program Projects (Grant No. 2025–MSLH–692).

Appendix A. Supplementary data

Supplementary data to this article can be found online at https://doi.org/10.1016/j.revpalbo.2026.105703.

Data availability

The authors confirm that all data necessary for supporting the scientific findings of this paper have been provided.

References

Ash, S.R., 1978. Geology, paleontology, and paleoecology of a late Triassic lake, western New Mexico. Brigham Young Univ. Geol. Stud. 25 (2), 1–95.

Bailey, I.W., Sinnott, E.W., 1915. A botanical index of Cretaceous and Tertiary climates. Science 41 (1066), 831–834. https://doi.org/10.1126/science.41.1066.831.

Bailey, I.W., Sinnott, E.W., 1916. The climatic distribution of certain types of angiosperm leaves. Am. J. Bot. 3 (1), 24–39. https://doi.org/10.1002/j.1537-2197.1916.tb05397.x.

Baird, A.S., Taylor, S.H., Pasquet-Kok, J., Vuong, C., Zhang, Y., Watcharamongkol, T., Scoffoni, C., Edwards, E.J., Christin, P.A., Osborne, C.P., Sack, L., 2021. Developmental and biophysical determinants of grass leaf size worldwide. Nature 592 (7853), 242–247. https://doi.org/10.1038/s41586-021-03370-0.

Barale, G., Thévenard, F., Zhou, Z., 1998. Discovery of *Nilssoniopteris* in the Middle Jurassic Yima Formation of Henan, Central China. Geobios 31 (1), 13–20. https://doi.org/10.1016/S0016-6995(98)80092-2.

Barnard, P.D.W., 1965. Flora of the Shemshak Formation. Part 1: Liassic Plants from Dorud. Rev. Ital. Paleontol. Stratigr. 71 (4), 1123–1168.

Blomenkemper, P., Bäumer, R., Backer, M., Abu Hamad, A., Wang, J., Kerp, H., Bomfleur, B., 2021. Bennettitalean leaves from the Permian of equatorial Pangea—the early radiation of an iconic Mesozoic gymnosperm group. Front. Earth Sci. 9, 652699. https://doi.org/10.3389/feart.2021.652699.

Bomfleur, B., McLoughlin, S., Vajda, V., 2018. Bennettitales. In: Krings, M., Harper, C.J., Cúneo, N.R., Rothwell, G.W. (Eds.), Transformative Paleobotany: Papers to Commemorate the Life and Legacy of. Academic Press, Amsterdam, pp. 1–30.
Bose, M.N., Banerji, J., 1984. The fossil floras of Kachchh. I. Mesozoic megafossils. Palaeobotanist 33, 1–189.
Boyd, A., 2000. Bennettitales from Early Cretaceous floras of West Greenland: Pterophyllum and *Nilssoniopteris*. Palaeontogr. Abt. B 255, 47–77.
Chen, F., Dou, Y.W., Huang, Q.S., 1984. Jurassic flora of West Hills, Beijing. Geological Publishing House, Beijing (in Chinese with English summary).
Chen, F., Meng, X.Y., Ren, S.Q., Wu, C.L., 1988. The Early Cretaceous Flora of Fuxin Basin and Tiefa Basin, Liaoning Province. Geological Publishing House, Beijing, 180 pp. (in Chinese with English summary).
Chen, W.Y., Su, T., Jia, L.B., Zhou, Z.-K., 2019. The relationship between leaf physiognomy and climate based on a large modern dataset: Implications for palaeoclimate reconstructions in China. Palaeogeogr. Palaeoclimatol. Palaeoecol. 527, 1–13 (in Chinese with English summary).
Cleal, C.J., Rees, P.M., 2003. The middle jurassic flora from Stonesfield, Oxfordshire, UK. Palaeontology 46 (4), 739–801. https://doi.org/10.1111/1475-4983.00319.
Cleal, C.J., Rees, P.M., Zijlstra, G., Cantrill, D.J., 2006. A clarification of the type of *Nilssoniopteris* Nathorst (fossil Gymnospermophyta, Bennettitales). Taxon 55 (1), 219–222. https://doi.org/10.2307/25065546.
Dai, J., Chen, W., Huang, L., Zhang, Y., 2023. Latest Neogene palaeoclimate variation in Yunnan, Southwest China, revealed by fossil leaf physiognomy. Acta Geol. Sin. (Engl. Ed.) 97 (4), 1268–1281. https://doi.org/10.1111/1755-6724.15012.
Deng, S.H., 1995. Early Cretaceous Flora of Huolinhe Basin, Inner Mongolia, China. Geological Publishing House, Beijing, 125 pp. (in Chinese with English summary).
Dilcher, D.L., 1974. Approaches to the identification of angiosperm leaf remains. Bot. Rev. 40 (1), 1–157. https://doi.org/10.1007/BF02858914.
Doludenko, M.P., Svanidze, T.I., 1969. The late Jurassic flora of Georgia. Trans. Geol. Inst. Acad. Sci. USSR 178, 1–116 (in Russian).
Farnsworth, A., Lunt, D.J., Robinson, S.A., Valdes, P.J., Roberts, W.H.G., Clift, P.D., Markwick, P., Su, T., Wrobel, N., Bragg, F., Kelland, S.-J., Pancost, R.D., 2019. Past East Asian monsoon evolution controlled by paleogeography, not CO_2. Sci. Adv. 5 (10), eaax1697. https://doi.org/10.1126/sciadv.aax1697.
Florin, R., 1933. Studien über die Cycadales des Mesozoikums nebst Erörterungen über die Spaltöffnungsapparate der Bennettitales. K. Sven. Vetenskapsakad. Handl. 12 (5), 1–134.
Givnish, T.J., 1987. Comparative studies of leaf form: assessing the relative roles of selective pressures and phylogenetic constraints. New Phytol. 106 (S1), 131–160. https://doi.org/10.1111/j.1469-8137.1987.tb04686.x.
Gordenko, N.V., 2008. Middle Jurassic flora of the Peski locality (Moscow Region): systematics, palaeoecology, and phytogeography. Paleontol. J. 42 (12), 1285–1382. https://doi.org/10.1134/S0031030108120010.
Harris, T.M., 1932. The fossil flora of Scoresby Sound East Greenland. Part 3: Caytoniales and Bennettitales. Meddr Grønland 85 (5), 1–114.
Harris, T.M., 1969. The Yorkshire Jurassic Flora. III. Bennettitales. Trustees of the British Museum (Natural History), London, pp. 1–186. https://doi.org/10.5962/bhl.title.118957.
Hay, W.W., 2008. Evolving ideas about the Cretaceous climate and ocean circulation. Cretac. Res. 29 (5–6), 725–753. https://doi.org/10.1016/j.cretres.2008.05.025.
Herman, A.B., Spicer, R.A., 2010. Mid-Cretaceous floras and climate of the Russian high Arctic (Novosibirsk Islands, Northern Yakutiya). Palaeogeogr. Palaeoclimatol. Palaeoecol. 295 (3–4), 409–422. https://doi.org/10.1016/j.palaeo.2010.02.034.
Herrera, F., Shi, G., Tsolmon, G., Ichinnorov, N., Takahashi, M., Crane, P.R., Herendeen, P.S., 2018. Exceptionally well-preserved Early Cretaceous leaves of *Nilssoniopteris* from central Mongolia. Acta Palaeobot. 58 (2), 135–148. https://doi.org/10.2478/acpa-2018-0008.
Huber, B.T., Norris, R.D., MacLeod, K.G., 2002. Deep-sea paleotemperature record of extreme warmth during the Cretaceous. Geology 30 (2), 123–126. https://doi.org/10.1130/0091-7613(2002)030<0123:DSPROE>2.0.CO;2.
Jenkyns, H.C., 2010. Geochemistry of oceanic anoxic events. Geochem. Geophys. Geosyst. 11, Q03004. https://doi.org/10.1029/2009GC002788.
Jones, D.L., 1993. Cycads of the World. Smithsonian Institution Press, Washington, D.C., 312 pp.
Kerp, H., 1990. The study of fossil gymnosperms by means of cuticular analysis. Palaios 5 (6), 548–569. https://doi.org/10.2307/3514861.
Kerp, H., Krings, M., 1999. Light microscopy of cuticles. In: Jones, T.P., Rowe, N.P. (Eds.), Fossil Plants and Spores: Modern Techniques. Geological Society, London, pp. 52–56.
Kiritchkova, A.I., Nosova, N.V., 2012. Jurassic continental deposits of the Middle-Caspian Basin. Part 2: Facies, Taphonomy, Interregional Correlations, Flora (Pinophyta: Pteridospermae, Cycadales, Bennettitales, Ginkgoales, Czekanowskiales, Coniferales). Trudy VSEGEI, St. Petersburg (in Russian with English abstract).
Kvaček, J., 1995. Cycadales and Bennettitales leaf compressions of the Bohemian Cenomanian, central Europe. Rev. Palaeobot. Palynol. 84 (3–4), 389–412. https://doi.org/10.1016/0034-6667(94)00093-Y.
Lambers, H., Chapin, F.S., Pons, T.L., 2008. Plant Physiological Ecology, 2nd ed. Springer, New York. https://doi.org/10.2307/176572. 604 pp.
Li, P.J., He, Y.L., Wu, X.W., Mei, S.W., Li, B.Y., 1988. Early and Middle Jurassic Strata and Their Floras from Northeastern Border of Qaidam Basin, Qinghai. Nanjing University Press, Nanjing, p. 231.
Li, X., 2017. Stratigraphic Distribution of Early Cretaceous *Nilssoniopteris* (Bennettitales) in Yanbian, NE China. Master's Thesis. Jilin University, Changchun.
Little, S.A., Kembel, S.W., Wilf, P., 2010. Paleotemperature proxies from leaf fossils reinterpreted in light of evolutionary history. PloS One 5 (12), e15161. https://doi.org/10.1371/journal.pone.0015161.
Lundblad, B., 1950. Studies in the Rhaeto-Liassic floras of Sweden. I. Pteridophyta, Pteridospermae, and Cycadophyta from the mining district of NW Scania. K. Sven. Vetenskapsakad. Handl. 1 (8), 1–82.
Mamay, S.H., 1976. Paleozoic origin of the cycads. U.S. Geol. Surv. Prof. Pap. 934, 1–48. https://doi.org/10.3133/pp934.
Masters, M.T., 1878. Zamia amplifolia. Gard. Chron., new series 10 (261), 810.
Na, Y.L., Sun, C.L., Dilcher, D.L., Wang, H.S., Li, T., Li, Y.F., 2014. Nilssoniopteris bingguensis sp. nov. (Bennettitales) from the Lower Cretaceous of northeast China. Int. J. Plant Sci. 175 (3), 369–381. https://doi.org/10.1086/673539.
Nathorst, A.G., 1909. Über die Gattung Nilssonia Brongn. mit besonderer Berücksichtigung schwedischer Arten. K. Sven. Vetenskapsakad. Handl. 43, 3–37.
Norstog, K.J., Nicholls, T.J., 1997. The Biology of the Cycads. Cornell University Press, Ithaca, 363 pp.
Palmer, E., Pitman, N., 1972. Trees of Southern Africa. A.A. Balkema, Cape Town, 3 vols.
Parrish, J.T., Daniel, I.L., Kennedy, E.M., Spicer, R.A., 1998. Paleoclimatic significance of Mid-Cretaceous floras from the Middle Clarence Valley, New Zealand. Palaios 13 (2), 149–159. https://doi.org/10.2307/3515486.
Peppe, D.J., Royer, D.L., Cariglino, B., Oliver, S.Y., Newman, S., Leight, E., Wright, I.J., 2011. Sensitivity of leaf size and shape to climate: global patterns and paleoclimatic applications. New Phytol. 190 (3), 724–739. https://doi.org/10.1111/j.1469-8137.2011.03698.x.
Pott, C., Van Konijnenburg-van Cittert, J.H.A., 2017. The type specimen of *Nilssoniopteris solitaria* (Phillips 1829) Cleal et P.M.Rees 2003 (Bennettitales). Acta Palaeobot. 57 (2), 177–184. https://doi.org/10.1515/acpa-2017-0008.
Pott, C., Krings, M., Kerp, H., 2007. The first record of *Nilssoniopteris* (Gymnospermophyta, Bennettitales) from the Carnian (Upper Triassic) of Lunz, Lower Austria. Palaeontology 50 (5), 1299–1318. https://doi.org/10.1111/j.1475-4983.2007.00704.x.
Ray, M.M., Rothwell, G.W., Stockey, R.A., 2014. Anatomically preserved early Cretaceous bennettitalean leaves: *Nilssoniopteris corrugata* n. sp. from Vancouver Island, Canada. J. Paleontol. 88 (5), 1085–1093. https://doi.org/10.1666/13-108.
Rudall, P.J., Bateman, R.M., 2019. Leaf surface development and the plant fossil record: stomatal patterning in Bennettitales. Biol. Rev. 94 (3), 1179–1194. https://doi.org/10.1111/brv.12497.
Sadovnikov, G.N., 1989. *Taeniopteris*, *Nilssoniopteris*, and *Nilssonia* in the Late Triassic flora of Iran. Paleontol. J. 23, 95–100.
Samylina, V.A., 1964. Mesozoic flora of the left bank of Kolyma river (Zyrjansky coal-bearing basin). Part I. Horsetails. Ferns. Cycads, Bennettitaleans. Trudy Bot. Inst. Akad. Nauk SSSR, Ser. 8, Paleobot. 5, 39–80.
Samylina, V.A., 1976. The Cretaceous Floras from Omusuckchan (Magadan District). Nauka, Leningrad (in Russian).
Schweitzer, H.-J., Kirchner, M., 2003. Die rhäto-jurassischen Floren des Iran und Afghanistans. 13. Cycadophyta III. Bennettitales. Palaeontogr. Abt. B 264 (1–16), 1–166.
Sellwood, B.W., Valdes, P.J., 2006. Mesozoic climates: general circulation models and the rock record. Sediment. Geol. 190 (1–4), 269–287. https://doi.org/10.1016/j.sedgeo.2006.05.013.
Spicer, R.A., Herman, A.B., 2010. The Late Cretaceous environment of the Arctic: a quantitative reassessment based on plant fossils. Palaeogeogr. Palaeoclimatol. Palaeoecol. 295 (3–4), 423–442. https://doi.org/10.1016/j.palaeo.2010.02.025.
Sun, K.Q., Shen, G.L., 1988. A new group of the plant kingdom: Progymnospermopsida. Fossils 1988 (1).
Sun, K.Q., Yang, X.L., 1988. Late Early Permian flora and its paleoclimatic significance in western Hubei. J. Lanzhou Univ. (Nat. Sci.) 24 (4).
Sze, H.C., 1936. Über einen Vorläufer von Pterophyllen in der unteren Shihhotze Serie in Shansi. Bull. Geol. Soc. China 15 (4), 467–472.
Sze, H.C., Li, X.X., 1963. Fossil Flora of China (Fasc. 2 Mesozoic Plants of China). Science Press, Beijing (in Chinese).
Tan, X., 2018. New Discovery of Early Cretaceous Fossil Plants and Palynoflora from Binggou Area, Jianchang County, Liaoning Province. Doctoral Dissertation. Jilin University, Changchun.
Tan, X., Feng, Y.H., Liang, F., Li, Y.F., Sun, C.L., Sun, G., 2026. Lower Cretaceous palynoflora from the Binggou Formation of Jianchang Basin, western Liaoning, NE China and its U–Pb zircon age. Cretac. Res. 179, 106247. https://doi.org/10.1016/j.cretres.2025.106247.
Taylor, T.N., Taylor, E.L., Krings, M., 2009. Paleobotany: The Biology and Evolution of Fossil Plants, second ed. Academic Press, Amsterdam. 1252 pp.
Tian, S.G., Zhang, Y.S., Li, Z.S., Wang, D.N., 2017. Redefinition of the Lower Cretaceous continental Fuxinian Stage and its stratotype section. Acta Geosci. Sin. 38 (3), 345–358. https://doi.org/10.3975/cagsb.2017.03.05.
Urban, T., Hardisty, F., 2013. Developing PAMS—a paleolocation web service. In: Proceedings of the International Cartographic Conference (ICC 2013), Dresden, Germany. Available at paleolocation.org.
Vázquez Torres, M., Sabato, S., Stevenson, D.W., 1986. *Ceratozamia euryphillidia* (Zamiaceae), a new species from Veracruz, Mexico. Brittonia 38 (1), 17–19. https://doi.org/10.2307/2807413.
Wang, Z.Q., 1984. Mesozoic flora. In: Palaeontological Atlas of North China (II). Geological Publishing House, Beijing, pp. 223–302.
Wang, X., Ding, Q.L., Santos, A.A., Wappler, T., 2022. *Nilssoniopteris longifolius* Chang from the Middle–Late Jurassic of China: implications for Bennettitales–insect interactions. Rev. Palaeobot. Palynol. 297, 104582. https://doi.org/10.1016/j.revpalbo.2021.104582.
Watson, J., Sincock, C.A., 1992. Bennettitales of the English Wealden. Monogr. Palaeontogr. Soc. 145 (588), 1–228.
Wei, W.Y., Sun, Y.W., Wang, Y.X., 2005. *Nilssoniopteris* from lower cretaceous Changcai Formation in Yanbian area of Jilin, China. Glob. Geol. 24 (1), 1–10.

Wolfe, J.A., 1995. Paleoclimatic estimates from Tertiary leaf assemblages. Annu. Rev. Earth Planet. Sci. 23 (1), 119–142. https://doi.org/10.1146/annurev.ea.23.050195.001003.

Wright, I.J., Dong, N., Maire, V., Prentice, I.C., Westoby, M., Díaz, S., Gallagher, R.V., Jacobs, B.F., Kooyman, R., Law, E.A., Leishman, M.R., Niinemets, Ü., Reich, P.B., Sack, L., Villar, R., Wang, H., Wilf, P., 2017. Global climatic drivers of leaf size. Science 357 (6354), 917–921. https://doi.org/10.1126/science.aal4760.

Yamada, T., Legrand, J., Nishida, H., 2009. Structurally preserved *Nilssoniopteris* from the Arida Formation (Barremian, Lower Cretaceous) of southwest Japan. Rev. Palaeobot. Palynol. 156 (3–4), 410–417. https://doi.org/10.1016/j.revpalbo.2009.04.006.

Zhang, Z.C., 1984. Palaeontological atlas of North China. 2. Mesozoic volume. Geological Publishing House, Beijing, pp. 191–192.

Zhang, F.F., Xin, C.L., Jiao, Z.P., Wei, L.X., Li, H., 2026. Two new species of *Nilssoniopteris* (Bennettitales) from the Middle Jurassic of Baojishan Basin, Gansu, northwestern China. J. Palaeogeogr. 15, 100389. https://doi.org/10.1016/j.jop.2026.100389.

Zhao, Y., 2018. Study on Cycadophytes from the Middle Jurassic flora of Sandaoling, Turpan-Hami Basin, Xinjiang, China. Ph.D. Thesis. China University of Geosciences, Beijing.

Zheng, S.L., Zhang, W., Zhang, Y., 1990. A new species of *Nilssoniopteris* from the Early Cretaceous of Hailar Basin. Acta Bot. Sin. 32 (6), 483–489.

Zhou, Z.Y., 1989. Late Triassic plants from Shaqiao, Hengyang, Hunan Province. Palaeontol. Cathayana 4, 131–197.

辽宁省教育厅高等学校基本科研项目
申请·评审书

（自然科学类）

项　目　名　称 辽西中生代本内苏铁类植物化石的全球三维重建与古气候协同模拟研究

一级学科代码与名称 0709　地质学

项　目　大　类 平台建设项目

专　项　类　别

项　目　负　责　人 谭笑

所　在　单　位（盖章） 沈阳师范大学

依　托　平　台 深时古生态与古环境科技创新重点实验室

填　表　日　期 2025 年 06 月 16 日

科研处

2025 年 6 月

一、项目组成员信息

项目负责人情况	姓　名	谭笑	性别	女	出生年月	1988 年 11 月
	学　位	博士研究生	技术职称	九级讲师	从事专业	古生物学与地层学
	个人成就 [　]	1、长江学者 2、教育部优秀人才 3、教育厅优秀人才 4、省百层次人才				
	联系电话	15940347715		E-mail	tanxiao1115@163.com	
	通讯地址	沈阳市沈北新区黄河北大街 253 号，110034				

二、项目组成人员情况（含主持人）

姓名	性别	出生年月	专业技术职务	一级学科	二级单位	课题分工	本人签名
谭笑	女	1988.11	讲师	地质学	古生物学院	项目总负责、实验及论文撰写	
王璐	女	1984.11	馆员	俄语语言学	辽宁古生物博物馆	馆藏标本收集整理与统计	
张曦	女	1981.09	馆员	历史学	古生物学院	文献收集、标本整理	
霍欣然	女	1985.07	中级馆员	语言学及应用语言学	古生物学院	文献收集、人员整合及文本校对	
何睿	男	1999.10	硕士研究生	生物学	古生物学院	数据整理及三维图制作	
王悦	女	2003.03	硕士研究生	生物学	古生物学院	文献收集，论文撰写，数据校对	
邢安琪	女	2004.06	本科生	地质学	古生物学院	实验处理，图版制作及数据校对	
秦露	女	2004.02	本科生	地质学	古生物学院	实验处理，图版制作及数据校对	
在校学生	博士生				硕士生	本科生	

辽 宁 省 教 育 厅

关于公布2025年度高校基本科研项目立项结果的通知

省内相关高校:

根据辽宁省教育厅《关于发布2025年度高校基本科研项目申报指引的通知》（辽教通〔2025〕186号）要求，经项目依托高校组织专家评审、省教育厅审核，现将立项结果公布如下:

一、全省高校共立项2569项（人文社科类项目1025项、自然科学类项目1544项），其中，自主选题项目1972项、科研平台建设项目149项、科技创新团队项目191项、创新发展项目257项。

二、各高校要按照《辽宁省高等学校基本科研项目暂行管理办法（试行）》（辽教办发〔2021〕28号）有关规定，加强项目监督与管理，自主开展基本科研项目绩效考核评价，自主确定结题标准，组织结题验收，并报教育厅备案。省属公办本科高校要按照《关于加强基本科研项目管理的通知》有关要求，严格自主管理，严格预算执行，严守财经纪律，加强绩效管理。

三、各高校于12月15日前向省教育厅报送基本科研项目年度

绩效报告。省教育厅将强化评价结果运用，将绩效评价结果作为项目调整、后续支持的重要依据。

附件：2025年度辽宁省教育厅高校基本科研项目立项名单（分发）

辽宁省教育厅

2025年8月29日

序号	状态标志	项目编号	项目名称	负责人	二级单位	所属年度	项目起止时间	总经费（万	人文/自然	项目类别
57	教育厅审核通过	LJ212510166008	辽宁本溪关门山北部早白垩世花岗岩成因及构造背景	白树崇	(018)古生物学院	2025	2025-07至2027-07	3.00	自然科学类	自主选题项目
58	教育厅审核通过	LJ212510166009	FeOOH-富缺陷镍基硫化物的导向构筑及电催化性能研究	毋妍妍	(014)物理科学与技术学院	2025	2025-07至2027-07	3.00	自然科学类	自主选题项目
59	教育厅审核通过	LJ212510166010	面向高速网络的实时细粒度流量测量研究	卜霄菲	(020)软件学院	2025	2025-07至2027-07	3.00	自然科学类	自主选题项目
60	教育厅审核通过	LJ212510166011	黑龙江嘉荫K-Pg界线火山事件地球化学示踪与源区识别	冯玉辉	(018)古生物学院	2025	2025-07至2027-07	3.00	自然科学类	自主选题项目
61	教育厅审核通过	LJ212510166012	全d族Heusler铁磁形状记忆合金成分-结构-性能优化的基础研究	李春梅	(014)物理科学与技术学院	2025	2025-07至2027-07	3.00	自然科学类	自主选题项目
62	教育厅审核通过	LJ212510166013	急诊医疗资源智能调度模型研究—面向处理时间动态变化的多目标协同优化	柏孟卓	(013)数学与系统科学学院	2025	2025-07至2027-07	3.00	自然科学类	自主选题项目
63	教育厅审核通过	LJ212510166014	基于摄动结点集的多元Birkhoff插值算法研究	崔凯	(013)数学与系统科学学院	2025	2025-07至2027-07	3.00	自然科学类	自主选题项目
64	教育厅审核通过	LJ212510166015	利他行为促进自我优势的神经计算机制：ERPs与漂移扩散模型的整合研究	孙洋	(005)教育科学学院	2025	2025-07至2027-07	3.00	自然科学类	自主选题项目
65	教育厅审核通过	LJ212510166016	油相富集与界面调控耦合的富硒菜籽油创新制备工艺	李嘉馨	(017)粮食学院	2025	2025-07至2027-07	3.00	自然科学类	自主选题项目
66	教育厅审核通过	LJ222510166001	柔性铋基钙钛矿光电检测器件的构建及光电性能增强机理研究	于吉	(014)物理科学与技术学院	2025	2025-07至2027-07	10.00	自然科学类	科技创新团队项目
67	教育厅审核通过	LJ222510166002	铜-共价有机框架催化C-N交叉偶联反应研究	杨晓博	(015)化学化工学院	2025	2025-07至2027-07	10.00	自然科学类	科技创新团队项目
68	教育厅审核通过	LJ222510166003	东北三省蜘蛛多样性调查、DNA数据库的建立与外来入侵物种鉴定	姚志远	(016)生命科学学院	2025	2025-07至2027-07	10.00	自然科学类	科技创新团队项目
69	教育厅审核通过	LJ222510166004	基于知识图谱和垂直大模型的多智能体对抗系统及其在智慧教育和巡视巡察中的应用	蔡云鹏	(013)数学与系统科学学院	2025	2025-07至2027-07	10.00	自然科学类	科技创新团队项目
70	教育厅审核通过	LJ222510166005	低碳化工与绿色生态交叉研究团队	赵震	(015)化学化工学院	2025	2025-07至2027-07	10.00	自然科学类	科技创新团队项目
71	教育厅审核通过	LJ232510166001	辽西中生代本内苏铁类植物化石的全球三维重建与古气候协同模拟研究	谭笑	(018)古生物学院	2025	2025-07至2027-07	10.00	自然科学类	科研平台建设项目
72	教育厅审核通过	LJ232510166002	多层物理信息神经网络深度学习及其改进算法的研究与应用	单佳文	(013)数学与系统科学学院	2025	2025-07至2027-07	10.00	自然科学类	科研平台建设项目
73	教育厅审核通过	LJ232510166003	未来高能对撞机上类轴子粒子与费米子耦合现象的探究	王晗	(014)物理科学与技术学院	2025	2025-07至2027-07	10.00	自然科学类	科研平台建设项目
74	教育厅审核通过	LJ232510166004	基于2型糖尿病小鼠模型探讨蛹虫草调控肝脏糖脂代谢的分子机制研究	王泽	(016)生命科学学院	2025	2025-07至2027-07	10.00	自然科学类	科研平台建设项目
75	教育厅审核通过	LJ232510166005	微生物发酵制备黑豆XOD肽类抑制剂及其构效关系研究	高育哲	(017)粮食学院	2025	2025-07至2027-07	10.00	自然科学类	科研平台建设项目
76	教育厅审核通过	LJ232510166006	刺萼龙葵耐旱促生内生菌的高效挖掘及耐旱作用机制解析	东雨竹	(016)生命科学学院	2025	2025-07至2027-07	10.00	自然科学类	科研平台建设项目
77	教育厅审核通过	LJ232510166007	CO2耦合烷烃制烯烃/芳烃Zn@ZSM-5双功能催化剂制备及反应机理研究	肖霞	(015)化学化工学院	2025	2025-07至2027-07	10.00	自然科学类	科研平台建设项目
78	教育厅审核通过	LJ232510166008	数据驱动的具身智能元技能学习与泛化感知决策研究	李航	(020)软件学院	2025	2025-07至2027-07	10.00	自然科学类	科研平台建设项目
79	教育厅审核通过	LJ242510166001	面向锂离子电池应用的二维层状多钒硼酸盐材料的可控合成与储能机制研究	刘芯辛	(015)化学化工学院	2025	2025-07至2027-07	5.00	自然科学类	创新发展项目
80	教育厅审核通过	LJ242510166002	分区管控导向的沈阳都市圈生态环境质量时空演化及驱动机制—基于改进型遥感生态指数的分区决策支持	施拓	(016)生命科学学院	2025	2025-07至2027-07	5.00	自然科学类	创新发展项目